PHYSICAL REVIEW E VOLUME 60, NUMBER 5 NOVEMBER 1999

Theoretical model of diatomic molecules interacting on a two-dimensional lattice

E. E. Mola,* V. Ranea, and J. L. Vicente
INIFTA, Instituto de Investigaciones Fisicoquímicas Teóricas y Aplicadas, Química Teórica, Sucursal 4,
Casilla de Correo 16, (1900) La Plata, Argentina

(Received 16 April 1999)

The coverage-dependent binding energy of interacting dimers is investigated using the lattice gas model. Dimers with distinguishable ends are assumed to interact if they occupy only nearest-neighbor lattice sites. The interaction energy between a pair of dimers will be repulsive if identical ends are in nearest-neighbor positions and attractive if they are not. The grand partition function is derived by using the Bethe approximation. The energy of the system of interacting dimers is evaluated as a function of the lattice coverage at different temperatures and pair interaction potentials. Under the same conditions the average number of all types of nearest-neighbors is evaluated. [S1063-651X(99)13010-1]

PACS number(s): 05.20.Gg, 82.65.Dp, 82.65.Jv

I. INTRODUCTION

Quite often surface reaction processes, molecular dissociation, thermal desorption spectra, and thermal conversion of admolecules binded to two neighboring sites have to be studied on a well-defined metal surface. These admolecules can be either homo- or heteronuclear diatomic molecules or even more complex admolecules such as acetylene or vinylidene. For simplicity, only a few examples where it might be necessary to consider admolecules binded to the two neighboring sites to understand experimental information will be mentioned.

The ability of Rh to efficiently dissociate NO makes it the most suitable metal for the removal of nitrogen oxides from automotive exhaust gases in catalytic converters [1]. Studies on the interaction of NO with single-crystal Rh(111) [2], Rh(100) [3], and Rh(110) [4] indicate that in general NO is adsorbed molecularly on rhodium at low temperatures, but it dissociates upon heating. At higher coverages, part of NO is desorbed molecularly and the remaining NO is decomposed to adsorbed N and O atoms. In general, step sites are considered to form stronger chemisorption bonds with adsorbates than terrace sites due to their higher unsaturated metal coordination [5]. Recently, this generalization has been observed to be insufficient. For example, studies of NO adsorption on Pd(112) demonstrated that even though the effect of step sites is to enhance the dissociation of NO, the adsorption of NO proceeds preferentially on terrace sites rather than on step sites [6]. It is clear that more fundamental understanding is required in order to comprehend how the surface structure can be utilized to control surface reactivity.

The transition metals Ni, Fe, Ru, and Co are known to hydrogenate CO to a wide range of products (see Ref. [7] and references cited therein). For this reason, studies of CO adsorption on single crystal surfaces of these materials have aroused much interest. Dissociation of CO is a prerequisite for the Fischer-Tropsch reaction to take place at the catalyst surface [8]. Among the low-index surfaces of hexagonally close-packed Co, the $(11\overline{2}0)$ [9] and $(10\overline{1}2)$ [10] surfaces are reported to be more active for dissociation of CO than the (0001) and $(10\overline{1}0)$ surfaces. However, at room temperature, CO is reported to be adsorbed molecularly on both these surfaces [10].

The theoretical model developed in Sec. II can also be applied to any type of molecules that require two neighboring sites in order to be adsorbed, as was postulated in the thermal conversion of acetylene to vynilidene on Rh(111) [11]. In Sec. III the average number of nearest-neighbor dimers either of the same type (*A* or *B* in Fig. 1) or a different type (*C* in Fig. 1) is evaluated. In Sec. IV the average interaction energy of the interacting bidimensional set of dimers is calculated.

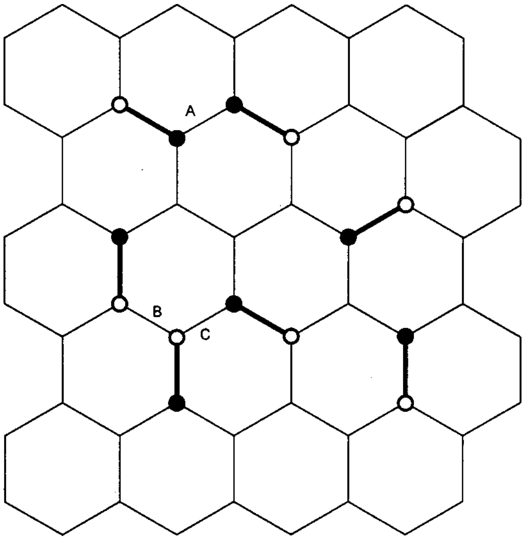

FIG. 1. Dimers with distinguishable ends (open and closed circles), distributed on a two-dimensional lattice space. There are three types of different nearest-neighbor interactions: *A* (closed and closed circles), *B* (open and open circles) and *C* (open and closed circles).

---

*Author to whom correspondence should be addressed. FAX: (0054) (221) (4254642).
Electronic address: eemola@infovia.com.ar

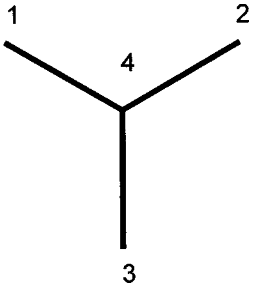

FIG. 2. Smallest cluster that can describe the interaction energy between dimers. The first shell sites are called 1, 2, and 3, and 4 is the central site.

II. THE PARTITION FUNCTION

Let us use the Bethe approximation to derive a partition function for the situation in which interacting dimers with distinguishable ends are distributed on a two-dimensional lattice space as the one shown in Fig. 1. A simple consideration of Fig. 1 immediately reveals that a sublattice composed of a ''central'' site and its three first shell sites (Fig. 2) is the smallest cluster that can describe the interaction energy between dimers. Let us call sites 1, 2, and 3 first shell sites and site 4, the central site. Let $\underline{n}_1$, n_2, n_3, and n_4 be the occupation number of sites 1, 2, 3, and 4, respectively, each element of which can assume the value 0 or 1 according to whether the corresponding site is vacant or occupied. The problem now is to determine for a given value of coverage (θ) the relative probability that the occupation numbers $\underline{n}_1$, n_2, n_3, and n_4 have a given set of values. Therefore, the degeneracy of arrangements that have the same energy has to be determined.

Let us now write down the energy of a particular configuration

$$E = aV_A + bV_B + cV_C + kV(\theta) - m\mu(\theta), \tag{1}$$

where a is the number of nearest-neighbor dimers on the sublattice, of type A (see Fig. 1), with potential energy of interaction V_A and b and c are the number of nearest-neighbor dimers of type B and C with potential energy of interaction V_B and V_C, respectively. $V(\theta)$ is the average interaction energy per particle on one of the first shell sites and the outer sites, $\mu(\theta)$ is the chemical potential, $\underline{k}$ is the number of occupied first shell sites aside from those associated with the dimers in the central sites (the number of dimers with an end outside the first shell sites), and $\underline{m}$ is the number of dimers brought from the outer sites to the sublattice and it can take the value $\underline{k}$ (if the central site is empty) and $\underline{k}+1$ (if the central site is occupied). Therefore, the grand partition function can be written as follows,

$$\Xi = \sum_{\text{all } n_i} g(n_1,\ldots,n_4)\,\eta_A^a \eta_B^b \eta_C^c \beta^k \lambda^m, \tag{2}$$

where $g(n_1,\ldots,n_4)$ is the multiplicity of those configurations that have the same energy; $\eta_A = \exp(-V_A/\mathrm{RT})$, $\eta_B = \exp(-V_B/\mathrm{RT})$, and $\eta_C = \exp(-V_C/\mathrm{RT})$; the terms in η take into account the pairwise interaction within the sublattice. Note that $\beta = \exp[-V(\theta)/\mathrm{RT}]$ and that $\lambda = \exp[-\mu(\theta)/\mathrm{RT}]$ is the absolute activity; the terms in λ take into account the change in chemical potential with the number of dimers brought into the sublattice. It is useful to define $\varepsilon = \lambda\beta$; therefore, Eq. (2) can be written as follows:

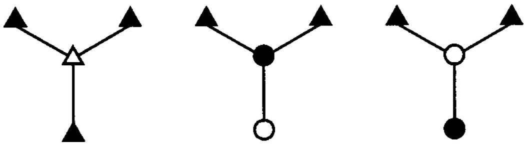

FIG. 3. The three basic configurations: open and closed circles are the ends of dimers, the full triangle is a lattice site that can be either vacant or occupied, and the open triangle is an always empty lattice site.

$$\Xi = \sum_{\text{all } n_i} g(n_1,\ldots,n_4)\,\eta_A^a \eta_B^b \eta_C^c \lambda^d \varepsilon^k, \tag{3}$$

where $\underline{d}$ can take the values 0 or 1 depending on whether the central site is empty or occupied, respectively.

In order to write down explicitly the grand partition function let us take into account the three basic configurations shown in Fig. 3; note that all of them are mutually exclusive. The lattice site indicated by an open triangle is always empty, and those indicated by a full triangle can be either vacant or occupied. Ends of dimers are indicated by open and closed circles. Table I shows the degeneracy value g for every possible set of exponents $\underline{a}$, $\underline{b}$, $\underline{c}$, $\underline{d}$, and $\underline{k}$ of Eq. (3) and for the three basic configurations. The contribution to the grand partition function from every basic arrangement, each

TABLE I. a, b, and c are the numbers of nearest-neighbor dimers on the sublattice, of type A, B, and C, respectively (see Fig. 1). d can take the values 0 or 1 depending on whether the central site is empty or occupied, respectively. k is the number of occupied first shell sites aside from that associated with the dimer in the central site (the number of dimers with an end outside the first shell sites). g is the multiplicity of those configurations that have the same energy. Configurations I, II, and III are shown in Fig. 3.

Configuration	(a)	(b)	(c)	(d)	k	g	Contribution to Ξ
I	0	0	0	0	0	1	1
	0	0	0	0	1	6	6ε
	0	0	0	0	2	12	$12\varepsilon^2$
	0	0	0	0	3	8	$8\varepsilon^3$
II	0	0	0	1	0	3	3λ
	1	0	0	1	1	6	$6\eta_A\varepsilon\lambda$
	0	0	1	1	1	6	$6\eta_C\varepsilon\lambda$
	2	0	0	1	2	3	$3\eta_A^2\varepsilon^2\lambda$
	0	0	2	1	2	3	$3\eta_C^2\varepsilon^2\lambda$
	1	0	1	1	2	6	$6\eta_A\eta_C\varepsilon^2\lambda$
III	0	0	0	1	0	3	3λ
	0	1	0	1	1	6	$6\eta_B\varepsilon\lambda$
	0	0	1	1	1	6	$6\eta_C\varepsilon\lambda$
	0	2	0	1	2	3	$3\eta_B^2\varepsilon^2\lambda$
	0	0	2	1	2	3	$3\eta_C^2\varepsilon^2\lambda$
	0	1	1	1	2	6	$6\eta_B\eta_C\varepsilon^2\lambda$

$$\Xi_I = (1+2\varepsilon)^3$$

$$\Xi_{II} = 3\lambda[1+\varepsilon(\eta_A+\eta_C)]^2$$

$$\Xi_{III} = 3\lambda[1+\varepsilon(\eta_B+\eta_C)]^2$$

of one is composed of 27 configurations shown on the right-hand side of Table I. Therefore, 81 distinguishable configurations can be identified in the sublattice.

Now the grand partition function can be written as

$$\Xi=(1+2\varepsilon)^3+3\lambda\{[1+\varepsilon(\eta_A+\eta_C)]^2 \\ +[1+\varepsilon(\eta_B+\eta_C)]^2\}. \tag{4}$$

Terms from excited states of the adsorbed particle are neglected in the partition function; this is a reasonable assumption for the systems and the experimental condition of interest in evaluating lateral interaction between adsorbed species.

Now, ε and λ have to be determined. To determine ε the ensemble average probability that a given first shell site, site 1 (Fig. 2) for instance, is occupied, is calculated. Using Bayes Theorem the average occupation value $\langle n_1\rangle$ of site 1 can be written as

$$\langle n_1\rangle=\sum_{i=1}^{3} P_i\langle n_1\rangle_i\,, \tag{5}$$

where i ranges over the three mutually exclusive basic configurations of Fig. 3, P_i is the joint probability of finding site 4 in a given configuration, and $\langle n_1\rangle_i$ is the average occupation number of site 1 in that particular configuration. Equation (5) can be written as follows:

$$\langle n_1\rangle=(1-\theta)\langle n_1\rangle_{\rm I}+\theta[\langle n_1\rangle_{\rm II}+\langle n_1\rangle_{\rm III}]. \tag{6}$$

Notice that θ is the *a-priori* probability of finding at random an occupied lattice site; if this event is successful, then the probability of finding one of its neighbors occupied (see Fig. 1) is no longer θ but $\frac{1}{3}$ or $(\frac{2}{3})$ θ in a first approximation, depending on whether it is occupied by the same dimer or by another one. Using Table I, $\langle n_1\rangle_i$ can be evaluated. Note that in configuration I, site 1 is never occupied by a dimer on the central site

$$\langle n_1\rangle_1=\frac{1}{3}\,\frac{6\varepsilon+24\varepsilon^2+24\varepsilon^3}{1+6\varepsilon+12\varepsilon^2+8\varepsilon^3}=\frac{2\varepsilon}{1+2\varepsilon}. \tag{7}$$

The average occupation number of site 1 in configurations II and III can be evaluated by different means. This evaluation can be simplified by taking into account that the contribution to the degree of occupation of site 1 by the dimer occupying the central site is $\frac{1}{3}$; therefore,

$$\langle n_1\rangle_{\rm II}+\langle n_1\rangle_{\rm III}=\langle t_1\rangle+\tfrac{1}{3}, \tag{8}$$

where $\langle t_1\rangle$ is the average occupation number of site 1 in configurations II plus III, by dimers that are not occupying the central site. Therefore, using Table I, and assuming $V_A=V_B$, $(\eta_A=\eta_B)$,

$$\langle t_1\rangle=\frac{2\varepsilon(\eta_A+\eta_C)}{3[1+\varepsilon(\eta_A+\eta_C)]} \tag{9}$$

and

$$\langle n_1\rangle_{\rm II}+\langle n_1\rangle_{\rm III}=\frac{1+3\varepsilon(\eta_A+\eta_C)}{3[1+\varepsilon(\eta_A+\eta_C)]}. \tag{10}$$

The overall average occupation number of site 1, $\langle n_1\rangle$, can now be evaluated from Eq. (6),

$$\langle n_1\rangle=\frac{2\varepsilon}{1+2\varepsilon}(1-\theta)+\frac{[1+3\varepsilon(\eta_A+\eta_C)]}{3[1+\varepsilon(\eta_A+\eta_C)]}\theta. \tag{11}$$

But site 1 is a typical site; therefore, $\langle n_1\rangle=\theta$, Then

$$3(\eta_A+\eta_C)(\theta-1)\varepsilon^2+(5\theta-3)\varepsilon+\theta=0 \tag{12}$$

and

$$\varepsilon=\{5\theta-3+[(5\theta-3)^2+12(\eta_A+\eta_C)\theta \\ \times(1-\theta)]^{1/2}\}/6(\eta_A+\eta_C)(1-\theta). \tag{13}$$

Equation (13) makes it possible to express ε as an independent function of V_A, V_B, V_C, θ, and T.

The probability that site 4 is occupied is given by

$$\Xi(n_4=1)/\Xi=\theta \tag{14}$$

because site 4 is also a typical site. From Eq. (14) and Table I we learn that

$$\Xi(n_4=1)=6\lambda[1+\varepsilon(\eta_A+\eta_C)]^2. \tag{15}$$

Using Eqs. (4), (13), (14), and (15), and after some algebra, the dependence of λ upon θ, V_A, V_B, V_C, and T is given by the following equation:

$$\lambda=\frac{(1+2\varepsilon)^3}{6[1+\varepsilon(\eta_A+\eta_C)]^2}\,\frac{\theta}{1-\theta}. \tag{16}$$

By solving Eqs. (13) and (16) at different coverages the grand partition function Ξ as a function of θ can be known. Note that η_A and η_C are external model parameters.

III. AVERAGE NUMBER OF NEAREST NEIGHBORS

The average number of nearest neighbors can be classified into two categories: (i) nearest neighbors of the same type $\langle n\rangle_{11}$ and (ii) nearest-neighbors of a different type $\langle n\rangle_{12}$. In order to evaluate both of them, let us focus our attention on configurations II and III. The average number of nearest neighbors of type $\langle n\rangle_{11}$ is equivalent to the average occupation number of first shell sites, in configuration II, by ends of dimers of the same type as the one occupying the central site,

$$\langle n\rangle_{11}=(6\varepsilon\lambda\eta_A+6\varepsilon^2\lambda\eta_A^2 \\ +6\varepsilon^2\lambda\eta_A\eta_C)/3\lambda[1+\varepsilon(\eta_A+\eta_C)]^2 \\ =2\varepsilon\eta_A/[1+\varepsilon(\eta_A+\eta_C)]. \tag{17}$$

The average number of nearest neighbors of type $\langle n\rangle_{12}$ is equivalent to the average occupation number of first shell sites occupied, in configuration II, by ends of dimers of a different type from the one occupying the central site,

$$\langle n\rangle_{12}=(6\varepsilon\lambda\eta_C+6\varepsilon^2\lambda\eta_C^2 \\ +6\varepsilon^2\lambda\eta_A\eta_C)/3\lambda[1+\varepsilon(\eta_A+\eta_C)]^2 \\ =2\varepsilon\eta_C/[1+\varepsilon(\eta_A+\eta_C)]. \tag{18}$$

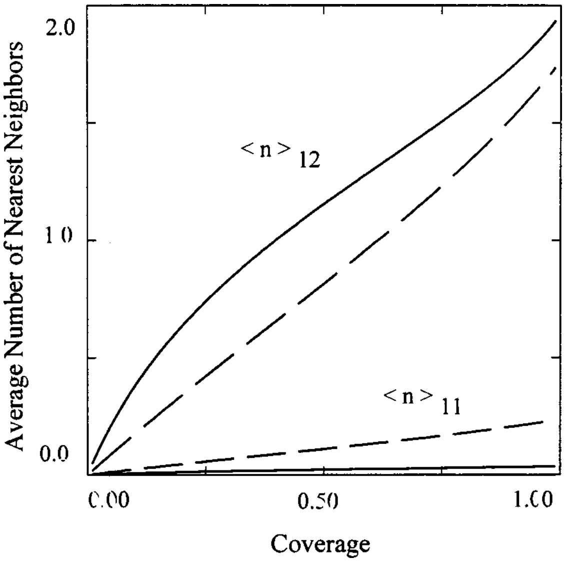

FIG. 4. Average number of nearest neighbors of type $\langle n\rangle_{11}$ and $\langle n\rangle_{12}$ vs coverage for different values of $V_A = V_B = -V_C$. $V_A = \mathrm{RT}$ (dashed line) and $V_A = 2\ \mathrm{RT}$ (solid line).

The dependence of $\langle n\rangle_{11}$ and $\langle n\rangle_{12}$ upon θ is given in Figs. 4 and 5 at four different ratios V/RT, and assuming a nearest-neighbor interaction

$$V_A = V_B = -V_C .$$

Note that as the coverage (θ) tends to one, ($\langle n\rangle_{11} + \langle n\rangle_{12}$) tends asymptotically to the value of 2.

IV. AVERAGE INTERACTION ENERGY

The average energy of the interacting bidimensional set of dimers $\langle E\rangle$ can be evaluated once the grand partition function is known from the following equation:

$$\langle E\rangle = (1-\theta)\langle E\rangle_{\mathrm{I}} + \theta(\langle E\rangle_{\mathrm{II}} + \langle E\rangle_{\mathrm{III}}), \tag{19}$$

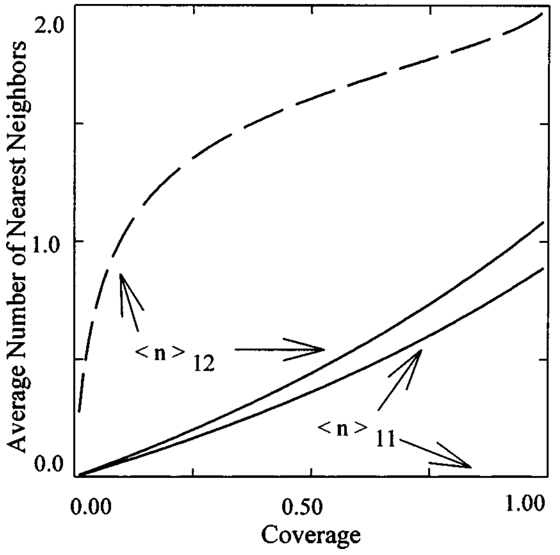

FIG. 5. Average number of nearest neighbors of type $\langle n\rangle_{11}$ and $\langle n\rangle_{12}$ vs coverage for different values of $V_A = V_B = -V_C$. $V_A = 4\ \mathrm{RT}$ (dashed line) and $V_A = 0.1\ \mathrm{RT}$ (solid line).

$$\begin{aligned}\langle E\rangle_{\mathrm{I}} &= [V(\theta)-\mu(\theta)](6\varepsilon+24\varepsilon^2+24\varepsilon^3)/(1+2\varepsilon)^3\\ &= [V(\theta)-\mu(\theta)]6\varepsilon/(1+2\varepsilon).\end{aligned} \tag{20}$$

Assuming that $V_A = V_B$, ($\eta_A = \eta_B$),

$$\begin{aligned}\langle E\rangle_{\mathrm{II}} + \langle E\rangle_{\mathrm{III}} = 2\{&V_A(6\eta_A\varepsilon\lambda + 6\eta_A^2\varepsilon^2\lambda + 6\eta_A\eta_C\varepsilon^2\lambda)\\ &+ V_C(6\eta_C\varepsilon\lambda + 6\eta_C^2\varepsilon^2\lambda + 6\eta_A\eta_C\varepsilon^2\lambda)\\ &- 3\mu(\theta)\lambda[1+\varepsilon(\eta_A+\eta_C)]^2 + [V(\theta)\\ &- \mu(\theta)](6\eta_A\varepsilon\lambda + 6\eta_C\varepsilon\lambda + 6\eta_A^2\varepsilon^2\lambda\\ &+ 6\eta_C^2\varepsilon^2\lambda + 12\eta_A\eta_C\varepsilon^2\lambda)\}\{6\lambda[1+\varepsilon(\eta_A\\ &+ \eta_C)]^2\}^{-1}\end{aligned} \tag{21}$$

$$\begin{aligned}&= \{6V_A\eta_A\varepsilon\lambda[1+\varepsilon(\eta_A+\eta_C)] + 6V_C\eta_C\varepsilon\lambda[1+\varepsilon(\eta_A\\ &\quad + \eta_C)] + [V(\theta)-\mu(\theta)]6\varepsilon\lambda(\eta_A+\eta_C)[1+\varepsilon(\eta_A+\eta_C)]\\ &\quad - 3\mu(\theta)\lambda[1+\varepsilon(\eta_A+\eta_C)]^2\}/3\lambda[1+\varepsilon(\eta_A+\eta_C)]^2,\end{aligned} \tag{22}$$

which can be rearranged as follows:

$$\begin{aligned}\langle E\rangle_{\mathrm{II}} + \langle E\rangle_{\mathrm{III}} = &\frac{2\varepsilon(\eta_A+\eta_C)}{[1+\varepsilon(\eta_A+\eta_C)]}[V(\theta)-\mu(\theta)]\\ &+ \frac{2\varepsilon\eta_A}{[1+\varepsilon(\eta_A+\eta_C)]}V_A\\ &+ \frac{2\varepsilon\eta_C}{[1+\varepsilon(\eta_A+\eta_C)]}V_C - \mu(\theta).\end{aligned} \tag{23}$$

Therefore,

$$\begin{aligned}\langle E\rangle = &\left\{\left[\frac{2\varepsilon(\eta_A+\eta_C)}{[1+\varepsilon(\eta_A+\eta_C)]}\right]\theta + \frac{6\varepsilon}{1+2\varepsilon}(1-\theta)\right\}\\ &\times[V(\theta)-\mu(\theta)] + \theta\frac{2\varepsilon\eta_A}{[1+\varepsilon(\eta_A+\eta_C)]}V_A\\ &+ \theta\frac{2\varepsilon\eta_C}{[1+\varepsilon(\eta_A+\eta_C)]}V_C - \theta\mu(\theta).\end{aligned} \tag{24}$$

Site 1 is a typical site; therefore,

$$\theta = (1-\theta)\langle n_1\rangle_{\mathrm{I}} + \theta(\langle n_1\rangle_{\mathrm{II}} + \langle n_1\rangle_{\mathrm{III}}). \tag{25}$$

From Eqs. (8) and (9) we learn that

$$\langle n_1\rangle_{\mathrm{II}} + \langle n_1\rangle_{\mathrm{III}} = \frac{1}{3} + \frac{2}{3}\,\frac{\varepsilon(\eta_A+\eta_C)}{[1+\varepsilon(\eta_A+\eta_C)]}. \tag{26}$$

Substituting Eq. (26) into Eq. (25) and after rearranging terms,

$$2\theta = \frac{2\varepsilon(\eta_A+\eta_C)}{[1+\varepsilon(\eta_A+\eta_C)]}\theta + \frac{6\varepsilon}{[1+2\varepsilon]}(1-\theta). \tag{27}$$

Substituting Eqs. (17), (18), and (27) into Eq. (24) we obtain

$$\langle E\rangle = \theta\{2[V(\theta)-\mu(\theta)] + \langle n\rangle_{11}V_A + \langle n\rangle_{12}V_C - \mu(\theta)\},$$

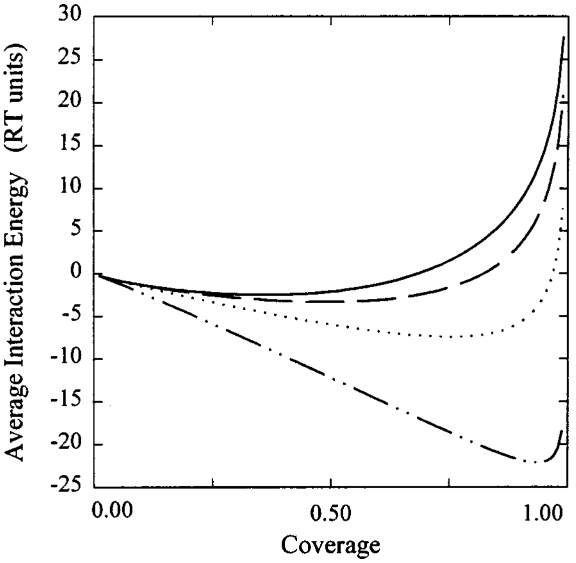

FIG. 6. Average interaction energy in units of RT vs coverage for different values of $V_A=V_B=-V_C$. $V_A=0.1$ RT (solid line), $V_A=$RT (long-dashed line), $V_A=2$ RT (dotted line), and $V_A=4$ RT (dash-dotted line).

from which the final expression for the average interaction energy can be obtained,

$$\langle E\rangle=\{2V(\theta)-3\mu(\theta)+\langle n\rangle_{11}V_A+\langle n\rangle_{12}V_C\}\theta. \quad (28)$$

V. CONCLUSIONS

The dependence of the average number of nearest neighbors to a particular end of a dimer on the interaction energy and coverage can be obtained in the present model. Figs. 4 and 5 show the average number of nearest neighbors of the same type, $\langle n\rangle_{11}$, or different type, $\langle n\rangle_{12}$, and how they depend on the interaction energy. This information is particularly useful to study the kinetics of surface reactions using approaches based on mean field approximations (see Fig. 6).

Surface reactions are of enormous importance for heterogeneous catalysis. Besides this practical importance one finds many complex and fascinating phenomena such as pattern formation and self-organization [12] as well as regular and irregular oscillations [13], even for apparently simple reactions over simple low-index single-crystal surfaces such as the $CO+O_2$/Pt(110) or CO+NO/Pt(100) reactions. Some of the mathematical models that have been proposed for oscillations in these reactions are of mean field type (Ertl and co-workers, Refs. [14,15] and King and co-workers Refs. [16,17]). Unfortunately, the effect of interaction energy upon the average number of nearest neighbors was not taken into account in those studies. We presume that the catalytic CO oxidation modeling by a mean-field approach can be greatly improved by using correlation effects on nearest-neighbor populations induced by interactions between admolecules. Although these interactions greatly influence the sticking probabilities of the molecules involved in the above-mentioned reactions [16,17], they were not taken into account in those analyses.

From the knowledge of $\langle n\rangle_{11}$, $\langle n\rangle_{12}$, $V(\theta)$, and $\mu(\theta)$, the average energy $\langle E\rangle$ of the interacting system of diatomic molecules can be derived as a function of coverage. The present approach can be adapted to study how the interactions affect the kinetics of a surface reaction. When coverage is higher or temperature is lower, the interactions within the adsorbed layer may become important to the reaction, since they determine the local structure of the surface and affect the adsorption of reactive molecules and the desorption of products, increasing or decreasing the rate of these processes.

ACKNOWLEDGMENTS

This research project was financially supported by the Consejo Nacional de Investigaciones Científicas y Técnicas, the Comisión de Investigaciones Cientificas de la Provincia de Buenos Aires, and the Universidad Nacional de La Plata. V. Ranea acknowledges financial support from the FOMEC program.

[1] K. C. Taylor, Catal. Rev. Sci. Eng. **35**, 457 (1993).
[2] H. J. Borg, JFC-JM Reijerse, R. A. van Santen, and J. W. Niemanstsverdriet, J. Chem. Phys. **101**, 10 052 (1994), and references therein.
[3] M. F. H. van Tol and B. E. Nieuwenhuys, Appl. Surf. Sci. **67**, 188 (1993).
[4] V. Schmatloch and N. Kruse, Surf. Sci. **269–270**, 488 (1992).
[5] K. Wandelt, Surf. Sci. **251–252**, 387 (1991).
[6] R. D. Ramsier, Q. Gao, H. Neergaard Waltenburg, and J. T. Yates, Jr., J. Chem. Phys. **100**, 6837 (1994).
[7] M. A. Vannice, in *Catalysis Science and Technology*, edited by J. R. Anderson and M. Boudart (Springer, Berlin, 1982), Vol. 3, p. 138.
[8] R. W. Joyner, J. Catal. **50**, 176 (1977).
[9] U. Bardi and G. Rovida, in *Structure and Reactivity of Surfaces*, edited by C. Monterra, A. Zecchina, and G. Costa (Elsevier, Amsterdam, 1989), p. 49.
[10] J. J. C. Geerlings, M. C. Zonnevylle, and C. P. M. de Groot, Surf. Sci. **241**, 315 (1991).
[11] D. C. Papageorgopoulos, Q. Ge, S. Nimmo, and D. A. King, J. Phys. Chem. B **101**, 1999 (1997).
[12] H. H. Rotermund, W. Engel, M. Kordesch, and G. Ertl, Nature (London) **343**, 355 (1990).
[13] G. Veser and R. Imbihl, J. Chem. Phys. **100**, 8492 (1994).
[14] R. Imbihl, M. P. Cox, G. Ertl, H. Müller, and W. Brenig, J. Chem. Phys. **83**, 1578 (1985).
[15] K. Krischer, M. Eiswirth, and G. Ertl, J. Chem. Phys. **96**, 9161 (1992).
[16] M. Gruyters and D. A. King, J. Chem. Soc., Faraday Trans. **93(17)**, 2947 (1997).
[17] M. Gruyters, T. Ali, and D. A. King, J. Phys. Chem. **100**, 14 417 (1996).